



Formation of magnetic moments in the cuprate superconductor $\text{Hg}_{0.8}\text{Cu}_{0.2}\text{Ba}_2\text{Ca}_2\text{Cu}_3\text{O}_{8+\delta}$ below T_c seen by NQR

H. Breitzke^{a,*}, I. Eremin^{b,c}, D. Manske^b, E.V. Antipov^d, K. Lüders^a

^a *Fachbereich Physik, Freie Universität Berlin, Arnimalle 14, D-14195 Berlin, Germany*

^b *Institut für Theoretische Physik, Freie Universität Berlin, D-14195 Berlin, Germany*

^c *Department of Physics, Kazan State University, 420008 Kazan, Russia*

^d *Department of Chemistry, Moscow State University, 119899 Moscow, Russia*

Received 4 November 2003; received in revised form 5 January 2004; accepted 18 February 2004

Available online 23 April 2004

Abstract

We report pure zero field nuclear magnetic resonance (NQR) measurements on the optimally doped three layer high- T_c -compounds HgBaCaCuO and $\text{HgBaCaCuO}(\text{F})$ with $T_c = 134$ K. Above T_c two Cu NQR line pairs are observed in the spectra corresponding to the two inequivalent Cu lattice sites. Below T_c the Cu NQR spectra show additional lines leading to the extreme broadened Cu NQR spectra at 4.2 K well known for the HgBaCaCuO compounds. The spin–lattice relaxation curves follow a triple exponential function with coefficients depend onto the saturation time (number of saturation pulses), whereas the spin–spin relaxation curve is described by a single exponential function. From the spin–lattice relaxation we deduced a complete removal of the Kramers degeneracy of the Cu quadrupole levels indicating that the additional lines are due to a Zeemann splitting of the $^{63/65}\text{Cu}$ lines due to the spontaneous formation of magnetic moments within the CuO layers. Below 140 K, the spectra are well fitted by a number of 6 $^{63/65}\text{Cu}$ line pairs. From the number of the Cu lines, the position of the lines relative to each other and the complete removal of the Kramers degeneracy we deduced an orientation of the magnetic moments parallel to the c -axis with magnitudes of the order of 1000 G. We also discuss the possible microscopic origin of the observed internal magnetic fields.

© 2004 Elsevier B.V. All rights reserved.

1. Introduction

A possible co-existence of antiferromagnetism and superconductivity remains one of the most interesting problem in high- T_c cuprates. Despite that in several theoretical scenarios of high- T_c superconductivity in cuprates the Cooper-pairing

arises due to an exchange of antiferromagnetic spin fluctuations present in the paramagnetic phase [1,2], it is commonly believed that bulk superconductivity and the antiferromagnetism do not co-exist in the cuprates at the same doping concentration and temperature. However, recently possible formation of antiferromagnetism below the superconducting transition temperature was found by several experimental techniques in underdoped $\text{YBa}_2\text{Cu}_3\text{O}_x$ and $\text{La}_{2-x}\text{Sr}_x\text{CuO}_4$ [3–6].

* Corresponding author.

E-mail address: breitzke@physik.fu-berlin.de (H. Breitzke).

The relatively small values of the observed magnetic moments [3,4] ($\sim 0.01\mu_B$, where μ_B is the Bohr magneton) have indicated an orbital rather than an electronic origin of the observed antiferromagnetism. Interestingly, some of these findings were interpreted in terms of the time-reversal symmetry breaking state [7] or *id*-density wave state [8] that may occur in the underdoped cuprates below the pseudogap formation temperature, T^* . Most recently, the time-reversal symmetry breaking below T^* has been indeed observed in underdoped $\text{Bi}_2\text{Sr}_2\text{-CaCu}_2\text{O}_{8+\delta}$ by means of the angle-resolved-photoemission spectroscopy (ARPES) [9].

Nuclear magnetic resonance (NMR) and nuclear quadrupole resonance (NQR) can be one of the most powerful tools to study the possible occurrence of the intrinsic antiferromagnetism in high- T_c cuprate superconductors. Very recently, the maximum in the transverse relaxation rate of Cu(2) nuclei observed in $\text{YBa}_2\text{Cu}_3\text{O}_7$ below T_c at $T = 35$ K was interpreted in terms of critical fluctuations of the *id*-density wave state [10]. A similar conclusion was drawn from the analysis of the spin-freezing processes in underdoped $\text{Y}_{2-x}\text{Ca}_x\text{Ba}_2\text{Cu}_3\text{O}_6$ and $\text{La}_{2-x}\text{Sr}_x\text{CuO}_4$ [11]. On the other hand, the NQR study provides a more direct prove for the formation of orbital magnetism since it is performed in zero magnetic field. Thus, the internal magnetic moments if they are present will result in the NQR line splitting. So far this splitting was not observed in high- T_c cuprates. Instead, one mainly observes anomalous broadened Cu NQR spectra at low doping [12–17]. Associating the broad Cu NQR spectra with doping inhomogeneities is leading to a few contradictions. The spectral width should depend on the preparation conditions and should have strongly decreased with improved preparation techniques developed in the past decade. Especially for the case of Hg-cuprates, that possess extremely broad NQR spectra, a dependency of the width of the NQR spectra on preparation conditions has never been reported. The second and more relevant reason against a doped inhomogeneity as the origin of the broad Cu NQR spectra is that it will spread the superconducting transition. An inhomogeneously distributed electric field gradient (EFG) is directly associated to an inhomogeneously distributed

charge density in the CuO layers. The charge density again is associated to the superconducting transition temperature. Thus, a distribution of spheres with distinct EFGs inside a crystal has to be associated to a distribution of T_c 's. If one estimates the distributions of T_c 's of HgBaCuO from the phenomenological model by Gippius et al. [18], the superconducting transition should be broadened by several ten K, what is clearly not the case.

The most interesting reason for additional NQR lines is the removing of the Kramers degeneracy of the Cu quadrupole levels due to a formation of magnetic fields at the Cu sites. Such magnetic fields may arise from an antiferromagnetic state formatting spontaneously below T_c .

Additional lines may also occur from impurities and Cu outside the CuO layers. However, lines from impurities should be visible at any temperature. If a line from an impurity becomes visible at a certain temperature it can be easily identified by their distinct relaxation times with respect to Cu inside CuO layers. Furthermore, the relaxation times of Cu inside the CuO layers are extremely short, in comparison with metallic Cu, and driven by antiferromagnetic fluctuations (AF) [19] inside the CuO layers, strongly decreasing with distance.

In this work, using NQR technique we present the first experimental evidence for the formation of the internal magnetic moments in the optimally doped three-CuO₂-layer $\text{Hg}_{0.8}\text{Cu}_{0.2}\text{Ba}_2\text{Ca}_2\text{Cu}_3\text{O}_{8+\delta}$ (Hg-1223) and $\text{Hg}_{0.8}\text{Cu}_{0.2}\text{Ba}_2\text{Ca}_2\text{Cu}_3\text{O}_{8+\delta}$ high-temperature cuprate superconductors (HTSC) below T_c ($T_c = 134$ K).

The synthesis of the samples is described in Ref. [20]. An impurity content of less than 5% within the sample was found from neutron powder diffraction and X-ray powder diffraction [20]. The real part of the ac-susceptibility is shown in Fig 1. Both samples possess different ways of preparation and types of dopants. Thus, any common properties have to be attributed to intrinsic properties of the superconducting state. In particular, we show that ^{63}Cu NQR-lines split below T_c due to a Zeeman splitting originating from the internal magnetic fields within the CuO₂-layers.

Our measurements were carried out on a home-built NQR spectrometer. The spectra have been recorded by point-by-point technique with a Hahn

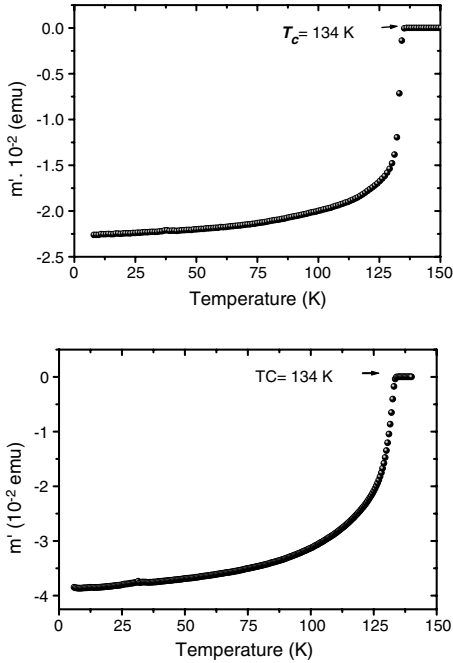


Fig. 1. Real part of the ac-susceptibility of the oxygenated sample (upper picture) of the fluorinated sample (lower picture). The superconducting transitions are relatively sharp and shows no further phases.

spin-echo pulse sequence with pulse lengths of 4 and 8 μs . The recovery of the longitudinal magnetization was measured by the method of saturation recovery. Various numbers of saturating pulses (from 3 to 101) have been used to study the dependency of the spin-lattice relaxation on the initial conditions. The decay of the transverse magnetization was measured by varying the pulse separation (τ) of the spin-echo sequence. In order to detect lines with strongly different T_2 times the spectra were scanned with first increasing pulse separation time τ_2 of the Hahn echo sequence. To detect lines with strongly different T_1 times the point to be measured was saturating by a saturating comp and after a time τ_1 measured by the Hahn spin-echo sequence.

The sample was housed in an unsealed sample container and completely immersed in liquid helium. Because heat-up effects have not been detected in NMR experiments in a gas flow cryostat at low temperatures, using comparable numbers of saturating pulses, heat-up effects can be excluded in our NQR experiment.

2. Zero field NQR

Nuclei with a spin $I \geq 1$ possess a quadrupole moment and interacting with an EFG. The EFG is described by the traceless tensor $V_{ij} = \frac{\delta^2 V}{\delta x_i \delta x_j}$. Since the EFG tensor is a traceless tensor, only the values V_{zz} and $V_{xx} - V_{yy}$ are needed to characterize the EFG tensor. The EFG tensor is commonly described by the values eq and η defined by the equations $eq = V_{zz}$ and $\eta = \frac{V_{xx} - V_{yy}}{V_{zz}}$. In high- T_c superconductors the elongated CuO octahedrons leading to the case of axial symmetry of the EFG at the Cu site, giving $\eta = 0$.

With the restriction to the case of axial symmetry of the EFG tensor, the interaction energy is defined by the well known Hamiltonian

$$H = \frac{e^2 q Q}{4I(2I-1)} (3I_z^2 - I^2) \quad (1)$$

with eQ the quadrupole moment of the nucleus. The eigenvalues of this unperturbed Hamiltonian are

$$E = \frac{e^2 q Q}{4I(2I-1)} (3m^2 - I(I+1)). \quad (2)$$

In general, there is a twofold degeneracy of the $\pm m$ eigenvalues corresponding to the symmetry of the nucleus charge distribution and of the EFG. For half integer spins a deviation from the EFGs rotational symmetry, $\eta \neq 0$, will not remove the degeneracy corresponding to Kramers theorem that states that the degeneracy of half integer spins can only completely be removed by a magnetic field.

For the case of nuclei like Cu with spin $I = 3/2$ the set of levels form a virtual two level system due to the Kramers degeneracy and only one transition will be observed. Note, that for this particular case, an observed Cu NQR line splitting can only be due to mesoscopic charge segregation and/or the appearance of a magnetic field at the nucleus site.

2.1. Zeeman perturbed NQR

The twofold degeneracy of the quadrupole level is corresponding to the fact, that turning the nuclei

end for end will leave the electrostatic energy unchanged. Applying a magnetic field at the nuclei will lower the symmetry of the system and lifting the degeneracy. In general the situation is described by adding a Zeeman term $H_z = \gamma_n B_0 h I_z$ to the unperturbed Hamiltonian [21] (1)

$$H = \frac{e^2 q Q}{4I(2I-1)} (3I_z^2 - I^2) + \gamma_n B_0 h I_z \quad (3)$$

and treating the problem in first order perturbation theory. The solutions can be divided into three cases: the magnetic field B_0 oriented in parallel, second perpendicular to the symmetry axis of the EFG, and third the magnetic field oriented with angles $\neq 0^\circ, 90^\circ$ with respect to the symmetry axis of the EFG. In the cases B_0 parallel to the symmetry axis, the mixing of the $|\pm 1/2\rangle$ level vanishes and only two lines are observed. In the case B_0 perpendicular to the symmetry axis the splitting of the $|\pm 3/2\rangle$ vanishes in first order and again two lines are observed. For case three the quadrupole levels split into four levels with a mixing of the $|\pm 1/2\rangle$ levels and four lines are observed. The three different cases are corresponding to different orientations of the magnetic field direction with respect to the symmetry axis of the EFG and can be distinguished by investigating the spin–lattice relaxation behavior under various initial conditions.

2.2. Spin–lattice Relaxation

In the simplest case, of a two level system, or a virtual two level system (degenerated system), the concept of spin temperature can be applied to the problem and the establishing of equilibrium magnetization $m(\infty)$ is described by the single exponential function $m(t) = m(\infty)(1 - \exp(-t/\tau))$. Thus, a line splitting in coincidence with a single exponential spin–lattice recovery function characterizes a line splitting due to a mesoscopic charge segregation and the absence of a magnetic field. The Kramers degeneracy is left unchanged and every line in the spectrum corresponds to a transition between degenerated $m = \pm 3/2, \pm 1/2$ levels. In case of unequally spaced levels (applied magnetic field) the system will come into internal equilib-

rium and into equilibrium with the lattice with distinct time constants. Furthermore, the recovery is not exponential and depend on the initial conditions i.e. the saturating time. In general, the recovery of the central transition of a four level system into equilibrium is described by a linear combination of three exponential functions

$$\frac{M(\infty) - M(t)}{M(\infty)} = \sum_{i=1}^3 a_i \exp(-W_i t) \quad (4)$$

whereas the a_i depend on the relaxation mechanism and saturating time. In order to extract the correct recovery law one has to know the dominant relaxation mechanism. In some particular cases the recovery law for spin–lattice relaxation can be given and are well known in magnetic resonance. For quadrupole splitting and magnetic relaxation for example a $I = 3/2$ nuclei like Cu the recovery of the central transition after short saturation time is described by the recovery law

$$\frac{M(\infty) - M(t)}{M(\infty)} = 0.1 \exp(-2W_1 t) + 0.9 \exp(-12W_2 t) \quad (5)$$

and

$$\frac{M(\infty) - M(t)}{M(\infty)} = 0.4 \exp(-2W_1 t) + 0.6 \exp(-12W_2 t) \quad (6)$$

for long saturating time [22,23]. If magnetic and quadrupole relaxation are allowed no analytic solution can be given. The situation in NQR is slightly different since $|\pm 1/2\rangle \leftrightarrow |\pm 3/2\rangle$, are excited, however, the general facts hold true that the spin–lattice relaxation is described by a multi exponential recovery law and that the component of the recovery law with the longer relaxation time will increase with increasing saturating time. This characteristic behavior can be utilized to distinguish not only between a magnetic and electric line splitting. In case of a magnetic line splitting it can be utilized to distinguish between the various orientations of the magnetic to the symmetry axis of the EFG tensor.

In case of the orientation of the magnetic field perpendicular to EFG's symmetry axis the $|\pm 3/2\rangle$ levels coincidence and the system consist of three

levels. The relaxation is now described by two transitions between these three levels and thus, in general, described by a two exponential recovery law. In the two other cases the recovery law is, in general, described by a three exponential law.

In most cases the time constants of the recovery law are close to each other and the three distinct exponential functions can hardly be resolved. In such a case one cannot distinguish a three exponential recovery law from a two exponential recovery law by a fitting procedure. However, three and two exponential recovery laws can be distinguished by their answers to various saturating times. In case of a two exponential recovery law varying the saturating time will only affect the coefficients of the individual exponential functions and not the time constants. If, however, a three exponential recovery trace is fitted with a two exponential recovery law, varying the saturating time will obtain different time constants for various saturating times.

Thus we safely conclude, that we can distinguish a line splitting due to a mesoscopic charge segregation and due to a removal of the Kramers degeneracy, by recording the spin–lattice relaxation curve under different initial conditions. Furthermore, in case of a removal of the Kramers degeneracy the orientation of the magnetic field with respect to the symmetry axis of the EFG can be deduced from the spin–lattice relaxation curve. Different initial conditions may established e.g. by using the method of saturation recovery and applying different numbers of saturation pulses. Under the condition of mesoscopic charge segregation, one expects a single exponential recovery independent of the number of saturating pulses. However, a removal of the Kramers degeneracy is leading to a multi exponential recovery curve depending on the initial conditions.

3. Results

3.1. Cu NQR Spectra

In Fig. 2 we show the evolution of $^{63/65}\text{Cu}$ spectra with temperatures from $T = 140$ to 4.2 K for the originated sample. The corresponding

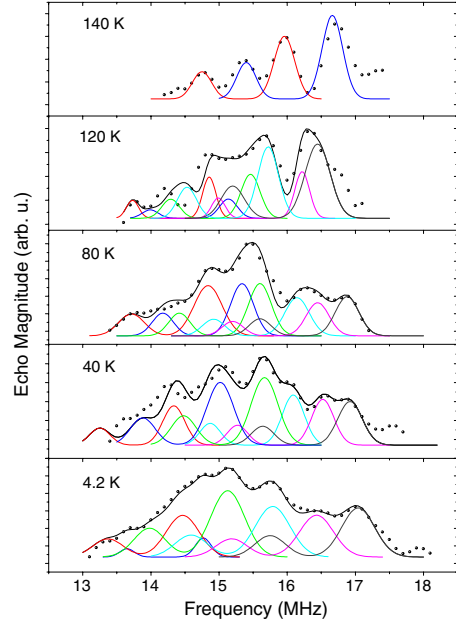


Fig. 2. Measured $^{63/65}\text{Cu}$ NQR spectra for the oxygenated sample at various temperatures (circles). Below T_c the spectra are described by six pairs of lines (solid curves) indicating the splitting of the resonance frequencies. For comparison also normal-state data are displayed where only two pairs of lines are present.

spectra for the fluorinated sample are shown in Fig. 3. For all temperatures the spectra lie between 13 and 19 MHz. Above T_c ($T = 140$ K) one clearly sees two pairs of lines corresponding to the resonance transition between $|\pm 3/2 \rangle \rightarrow |\pm 1/2 \rangle$ quadrupole levels of the copper nuclear spins belonging to the inner and outer CuO_2 -layers. The spectra above T_c are fitted with Eq. (7) according to the various natural abundance and quadrupole moments of the $^{63/65}\text{Cu}$ isotopes.

$$Y = y_0 + A \cdot \exp\left(\frac{(x - x_0)^2}{2W^2}\right) + 2.3 \cdot A \cdot \exp\left(\frac{(x - 1.082 \cdot x_0)^2}{2 \cdot (1.082 \cdot W)^2}\right). \quad (7)$$

In accordance with previous NMR studies the pair of lines with higher frequency and larger intensity corresponds to the two outer CuO_2 -layers while the other pair of lines to the inner one [24]. Most importantly, the $^{63/65}\text{Cu}$ NQR of both sample exhibit the same evolution with temperature.

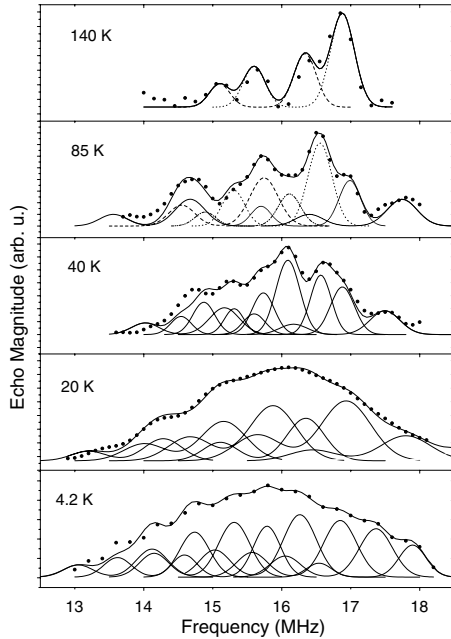


Fig. 3. Measured $^{63/65}\text{Cu}$ NQR spectra for the fluorinated sample at various temperatures (circles). Below T_c and above 4.2 K the spectra are described by six pairs of lines (solid curves). At 4.2 K the spectrum can only satisfactory be fitted with eight pairs of lines.

Below T_c the copper NQR spectra are strongly broadened and cannot be fitted with two pairs of lines. Instead, a good agreement can be achieved by using six pairs of lines according to Eq. (7). It is important to note that the spectra are fitted with line pairs of fixed relative frequency spacings and relative intensities. This restricts the degree of freedom of the fits despite their large number of free parameters. If one, for example, fits the lower end of the spectrum and subsequently the upper end the resulting curve has to fit the middle part of the spectrum. Under this condition the resulting fits are reliable if the measured spectra exhibits pronounced peaks.

The occurrence of additional lines within the spectrum is not an evidence for a line splitting. These lines may arise from impurities, Cu outside the CuO layers or Cu from distinct doped phases. However, additional lines from impurities should be clearly visible above T_c within the spectrum and should strongly differ from their relaxation times.

The same can be stated for lines arising from distinct doped phases.

3.2. Spin–lattice relaxation

The spin–lattice relaxation time of Cu in superconducting high- T_c s is extremely short and driven by antiferromagnetic (AF) fluctuation within the CuO layers [19]. The spin–lattice relaxation times of Cu and Hg, in HgBaCuO for example, differ by two orders of magnitudes [19]. From the ratio $\gamma(\text{Cu})/\gamma(\text{Hg})$ of their gyromagnetic ratios one would expect a ratio of the spin–lattice relaxation times of the order of two. The difference is explained by the AF fluctuations within the CuO layers strongly decreasing with distance. As demonstrated by Figs. 4 and 5 the relaxation times

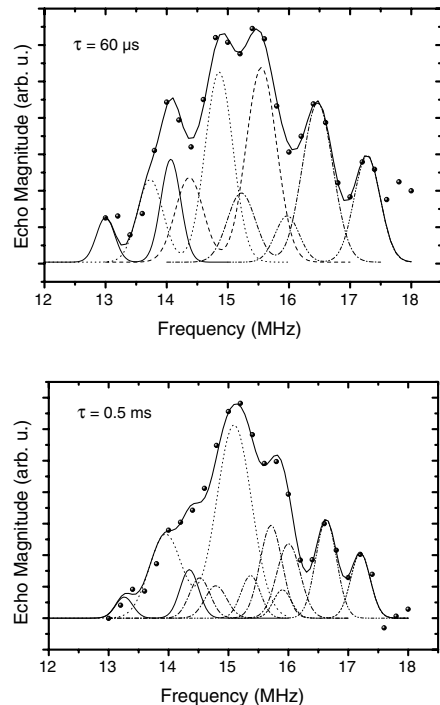


Fig. 4. Measured $^{63/65}\text{Cu}$ NQR spectra at 4.2 K under various conditions for the originated sample. In the upper picture the pulse spacing of the spin–echo sequence was increased from 23 to 60 μs . In the lower picture the frequency range to be measured was first saturated by a saturating comp and after 0.5 ms the recovered magnetization was probed by a spin–echo sequence. The relaxation times vary smoothly within the spectrum.

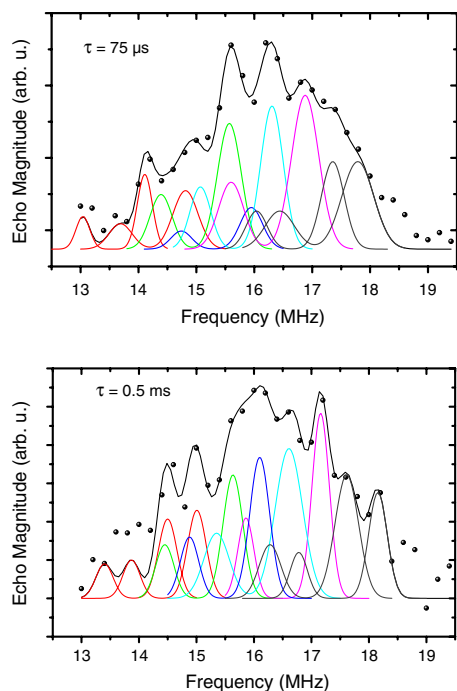


Fig. 5. Measured $^{63/65}\text{Cu}$ NQR spectra at 4.2 K under various conditions for the fluorinated sample. In the upper picture the pulse spacing of the spin-echo sequence was increased from 23 to 75 μs . In the lower picture the frequency range to be measured was first saturated by a saturating comp and after 0.5 ms the recovered magnetization was probed by a spin-echo sequence. The relaxation times vary smoothly within the spectrum.

vary only smoothly within the spectra what can be interpreted as a proof for Cu inside CuO layers as the origin of the additional lines. Furthermore, these lines have to belong to the same superconducting phase as proofed by the sharp superconducting transition (Fig. 1). From the doping dependency of the Cu NQR frequency in the one layer superconductor $\text{HgBa}_2\text{CuO}_4$ [18] one can estimate the difference in T_c of phases possessing a Cu NQR frequency difference of 1 MHz to be several ten Kelvin what is clearly not seen in Fig. 1. So far it is plausible that the additional lines are due to a line splitting of the two NQR lines visible at 140 K. In order to distinguish between the possible origins of the observed splitting we present in Fig. 6 the ^{63}Cu spin-lattice and spin-spin relaxation curves measured at $\nu = 16.6$ MHz. Various numbers of saturating pulses were applied

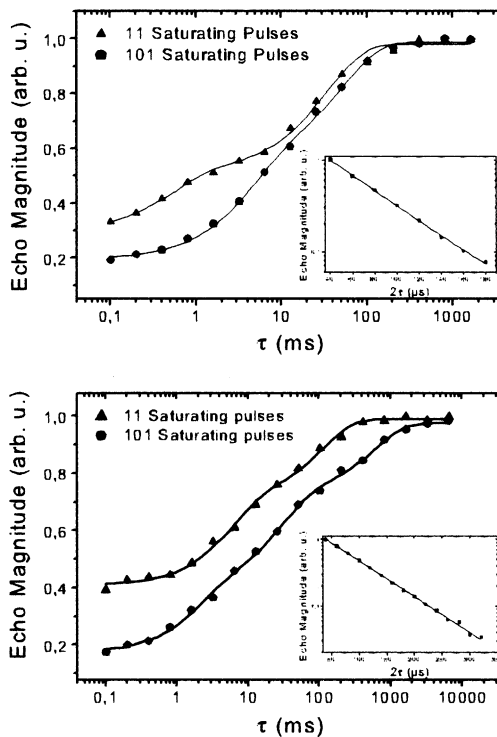


Fig. 6. ^{63}Cu spin-lattice relaxation curves at $\nu = 16.6$ MHz for the oxygenated (upper picture) and fluorinated (lower picture) sample. The relaxation curve for 11 and 101 saturating pulses are denoted by squares and circles, respectively. The solid curves in the upper picture denoting fits using a two exponential function. The relaxation process in the lower picture can be fitted with a two exponential function for 11 saturating pulses and a three exponential function for 101 saturating pulses. The ^{63}Cu transverse relaxation is purely single exponential for both samples (see insets).

according to the dependency of the relaxation process illustrated in Section 2.2. As seen in Fig. 6 the spin-lattice relaxation follows a two exponential behavior strongly depending on the number of saturating pulses. The deduced relaxation times are shown in Table 1. It is remarkable that the deduced relaxation times depend on the initial conditions. As discussed in Section 2.2 this can be understood under the assumption of three exponential relaxation behavior fitted with a two exponential recovery law. This assumption is supported by the Cu spin-lattice relaxation in the fluorinated sample which is shown in the lower picture of Fig. 6. Increasing the number of

Table 1

^{63}Cu Spin–lattice relaxation times of the oxygenated sample $T_1^{(1)}$ and $T_1^{(2)}$ and the according coefficients a_1 and a_2 of the two exponential fits according to Fig. 6 for different numbers of saturating pulses

Pulses	a_1	$T_1^{(1)}$ (ms)	a_2	$T_1^{(2)}$ (ms)
11	0.22(2)	0.6(2)	0.46(2)	35(4)
101	0.44(3)	4.3(5)	0.35(3)	56(4)

Table 2

^{63}Cu Spin–lattice relaxation times of the fluorinated sample $T_1^{(1)}$, $T_1^{(2)}$ and $T_1^{(3)}$ and the according coefficients a_1 , a_2 and a_3 of the two and three exponential fits according to Fig. 6 for different numbers of saturating pulses

Pulses	a_1	$T_1^{(1)}$ (ms)	a_2	$T_1^{(2)}$ (ms)	a_3	$T_1^{(3)}$ (ms)
11	0.28(2)	5.7(8)	0.29(2)	108(15)	–	–
101	0.23(3)	2.2(4)	0.32(2)	30(5)	0.26(2)	590(90)

saturating pulses reveals a third relaxation function. Exactly such a behavior is expected from the relaxation theory and Eqs. (5) and (6). The coefficient of the component with the longer relaxation time increases with increasing saturating time (Table 2). Furthermore, the transverse relaxation is purely single exponential. Thus, a formation of the internal magnetic fields as an origin of the observed splitting can be concluded.

4. Deduced magnetic fields

A magnetic field present at the copper nuclei will split the two line pairs observed at 140 K into four pairs of lines. However, the spectra cannot be fitted with four pairs of lines within the whole temperature range. Instead, a reasonable agreement could be achieved by using six pairs of lines. This can be understood by the following assumption. If both outer CuO_2 -layers would not be equal below T_c , the NQR spectrum will consist of three pairs of lines. In this case both outer CuO_2 -layers differ with respect to their EFG. If these three NQR line pairs split due to the formation of magnetic moments in the CuO_2 -layers, the spectrum will consist of six pairs of lines. This is indeed observed. One may argue that an electrical inequality is against the crystal symmetry because the inner CuO layer is a symmetry layer. However, the symmetry is immediately broken when a magnetic field appears in the inner layer with a

direction parallel to the c -axis. So far the rules of symmetry are not violated. As discussed above the deduced three-exponential spin–lattice relaxation is as an indicator for exactly that field direction. It can be stated that the interpretation of the data is consistent.

Associating the line pairs to the CuO_2 -layers has been done by comparing the line intensities at 4.2 K under the condition that the sum of the intensities of the outer CuO_2 -layers lines have to be twice of the intensity of the inner CuO_2 -layer. Subsequently, the magnetic field has been deduced from the equation $H = \Delta\nu/2\gamma$, with γ as the gyromagnetic ratio of the ^{63}Cu nucleus and $\Delta\nu$ as the frequency spacing of the ^{63}Cu lines. The results are shown in Fig. 7. The values of the internal magnetic fields vary from the inner to the outer CuO_2 -layer and the maximum field is of order of 700 G for the oxygenated sample and 1500 G for the fluorinated sample.

Now we would like to discuss the possible origin of these internal magnetic fields. We can exclude the presence of the water as a source of the weak antiferromagnetism in the CuO_2 -plane as was suggested recently [25], since our measurements were performed on fresh samples. Furthermore, the values of the deduced magnetic fields in our case is much larger than those measured in the water-inserted YBaCuO compounds. Similarly, the formation of the time-reversal symmetry breaking state [7] can be excluded since it would not give a magnetic moment on the copper site.

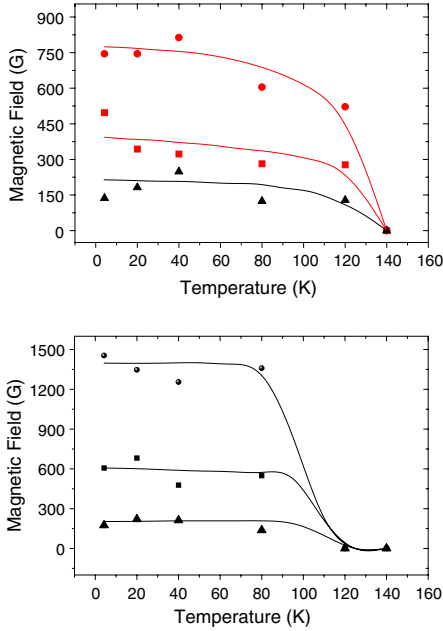


Fig. 7. Temperature dependence of the extracted magnetic field for the different CuO_2 -layers (upper picture: oxygenated sample, lower picture: fluorinated sample). Circles and squares: outer layers, triangles: inner layer. The solid curves are guides to the eyes.

Note that one of the most probable scenarios for the microscopical origin of the observed magnetic fields could be the formation of *id*-density wave [8] or the short-range antiferromagnetic spin correlations remnant from the parent antiferromagnetic compounds and suppressed by the doped carriers. In the first case, one expects that the *id*-density wave (DDW) state with the $d_{x^2-y^2}$ -wave symmetry of the order parameter ($\eta_{\mathbf{k}} = i\frac{\eta_0}{2}(\cos k_x - \cos k_y)$) is formed around the pseudogap formation temperature T^* which for optimally-doped cuprates is close to T_c . Below T^* the staggered orbital currents are formed due to the imaginary character of the order parameter [26]. Furthermore, these currents induce the formation of the internal magnetic moments perpendicular to the CuO_2 -layer and their magnitudes are increasing upon decreasing temperature.

These magnetic moments perpendicular to the CuO_2 -layer will remove the Kramers degeneracy resulting in an unequally spaced level system characterized by a three-exponential spin-lattice

relaxation. A three-exponential spin-lattice relaxation cannot occur if the magnetic moments are in parallel to the CuO_2 -layer (which would be the case if the moments are originated from the remnant antiferromagnetic phase), provided the Zeeman energy is small enough not to split the $|\pm 3/2\rangle$ levels, i.e. first order perturbation theory is valid [27]. Comparing the field strengths found in this work to field strengths of first order splittings found in $\text{YBa}_2\text{Cu}_{3-z}\text{Al}_z\text{O}_{6+0.18}$ [28] seems to confirm the validity of the first order perturbation theory. Thus, assuming magnetic moments parallel to the CuO_2 -layer may explain the line splitting, however, can hardly explain the three-exponential spin-lattice recovery.

In the DDW scenario the value of the internal magnetic fields, DDW gap, and pseudogap formation temperature will be ultimately related to each other. In particular, using the relation obtained earlier [29] between the orbital currents and the DDW order parameter one gets $j_0 = \frac{4et}{\hbar} \eta_0$ where $t = 250$ meV is a hopping integral between nearest neighbors in the CuO_2 -plane and $J = 120$ meV is a corresponding superexchange interaction. One can easily estimate the values of the internal magnetic fields as $H_{\text{int}} = j(T=0)/cr$ ($r \approx 2$ Å). For example, taking the value of $\eta_0 = 30$ meV one obtains H_{int} of the order of 100 G. This value qualitatively agrees with those we obtain from the splitting of NQR lines at $T = 4.2$ K for the inner CuO_2 -layer. Note, the corresponding internal magnetic moments are of the order $l_c \approx 0.03 \mu_B$ that agrees with neutron scattering experiments [3]. On the other hand, despite some consistency we notice several problems. Therefore, further theoretical and experimental studies are needed in order to identify the microscopical origin of the internal magnetic fields. For example, the magnitude of the magnetic fields varies and enhances for the outer CuO_2 -layers in comparison to the inner CuO_2 -layer. This seems to contradict the *id*-density wave scenario, since it is expected that the doping concentration of the holes in the inner and the outer CuO_2 -layers are different and the latter are more doped. Then, the magnitude of the magnetic moments should be smaller there. This is in contrast to our observation.

5. Summary

In summary, we perform copper NQR measurements in the optimally-doped three-CuO₂-layer Hg-1223 high-temperature cuprate superconductor. We show that the ⁶³Cu NQR-lines in all three CuO₂-layers broaden below T_c due to a Zeeman splitting originating from the internal magnetic fields (magnetic moments) within the CuO₂-layers. Analyzing the NQR spectra we obtain the values of the internal magnetic fields within the CuO₂-layer. For the outer CuO₂-layers its values vary from 400 to 1400 G, respectively, while for the inner CuO₂-layer its value is approximately 200 G. Note, the formation of *id*-density wave or short-range antiferromagnetic spin correlations remnant from the parent antiferromagnetic compounds and suppressed by the doped carriers could be possible scenarios as a microscopic origin of the observed fields.

D.M. and I.E. are supported by the INTAS Grant No. 01-0654.

References

- [1] A.V. Chubukov, D. Pines, J. Schmalian, in: K.H. Bennemann, J.B. Ketterson (Eds.), *Handbook of superconductivity: Conventional, High-Transition Temperature, and Novel Superconductors*, 1, Springer-Verlag, Berlin, 2002, p. 495.
- [2] D. Manske, I. Eremin, K.H. Bennemann, in: K.H. Bennemann, J.B. Ketterson (Eds.), *Handbook of Superconductivity: Conventional High-Transition Temperature, and Novel Superconductors*, Springer-Verlag, Berlin (in press).
- [3] H. Mook, P. Dai, F. Dogan, *Phys. Rev. B* 64 (2001) 012502.
- [4] Y. Sidis, C. Ulrich, P. Bourges, et al., *Phys. Rev. Lett.* 86 (2001) 4100.
- [5] J.E. Sonier, J.H. Brewer, R.F. Kiefl, R.I. Miller, G.D. Morris, C.E. Stronach, J.S. Gardner, S.R. Dunsiger, D.A. Bonn, W.N. Hardy, R. Liang, R.H. Heffner, *Science* 292 (2001) 1692; R.I. Miller, R.F. Kiefl, J.H. Brewer, J.E. Sonier, J. Chakhalian, S. Dunsiger, G.D. Morris, A.N. Price, D.A. Bonn, W.H. Hardy, R. Liang, *Phys. Rev. Lett.* 88 (2002) 137002.
- [6] B. Lake, G. Aeppli, K.N. Clausen, D.F. McMorrow, K. Lefmann, N.E. Hussey, N. Mangkorntong, M. Nohara, H. Takagi, T.E. Mason, A. Schröder, *Science* 291 (2001) 1759.
- [7] C.M. Varma, *Phys. Rev. Lett.* 83 (1999) 3538.
- [8] S. Chakravarty, R.B. Laughlin, D.K. Morr, Ch. Nayak, *Phys. Rev. B* 63 (2001) 094503.
- [9] A. Kaminski, S. Rosenkranz, H.M. Fretwell, J.C. Campuzano, Z. Li, H. Raffy, W.G. Cullen, H. You, C.G. Olson, C.M. Varma, H. Höchst, *Nature (London)* 416 (2002) 610.
- [10] M.V. Eremin et al., *Pis'ma Zh. Eksp. Teor. Fiz.* 73 (2001) 609; M.V. Eremin et al., *JETP Lett.* 73 (2001) 540.
- [11] M. Eremin, A. Rigamonti, *Phys. Rev. Lett.* 88 (2002) 037002.
- [12] Y. Kohori, K.-I. Ueda, T. Kohara, *Physica C* 185–189 (1991) 1187.
- [13] K. Fujiwara, Y. Kitaoka, K. Asayama, H. Sasakura, S. Minamigawa, K. Nakahigashi, S. Nakanishi, M. Kogachi, N. Fukuoka, A. Yanase, *J. Phys. Soc. Jpn* 58 (1989) 380.
- [14] K. Fujiwara, Y. Kitaoka, K. Ishida, K. Asayama, Y. Shimakawa, T. Manako, Y. Kubo, *Physica C* 184 (1991) 207.
- [15] T. Oashi, K. Kumagai, H. Nakajima, M. Kikuchi, Y. Syono, *Physica C* 161 (1989) 367.
- [16] I.E. Lipinski, A.V. Zalesky, A.P. Levanyuk, G.S. Mironova, E.M. Smirnovskaya, *Physica C* 168 (1990) 291.
- [17] K. Asayama, Y. Kitaoka, *Z. Naturforsch.* 45a (1990) 405.
- [18] A.A. Gippius, E.N. Morozova, E.V. Antipov, A.M. Abakumov, M.G. Rozova, G. Buntkowsky, O. Klein, *Phys. Rev. B* 61 (2000) 14370.
- [19] B.J. Suh, F. Borsa, J. Sok, D.R. Torgeson, M. Xu, *Phys. Rev. B* 54 (1996) 545.
- [20] K.A. Lokshin, D.A. Pavlov, S.N. Putilin, et al., *Phys. Rev. B* 63 (2001) 064511.
- [21] C.P. Slichter, *Principles of Magnetic Resonance*, third ed., Springer-Verlag, Berlin, 1990.
- [22] E.R. Andrew, D.P. Tunstall, *Proc. Phys. Soc. London* 78 (1961) 1.
- [23] A. Narath, *Phys. Rev.* 162 (1967) 3159.
- [24] M.-H. Julien et al., *Phys. Rev. Lett.* 76 (1996) 4238.
- [25] A.V. Dooglav, A.V. Egorov, I.R. Mukhamedshin, A.V. Savinkov, H. Alloul, J. Bobroff, W.A. MacFarlane, P. Mendels, G. Collin, N. Blanchard, P.G. Picard, P.J.C. King, J. Lord, cond-mat/0309698 (unpublished).
- [26] J.B. Marston, I. Affleck, *Phys. Rev. B* 39 (1989) 11538.
- [27] A. Abragam, *The Principles of Nuclear Magnetism*, Oxford University Press, 1973.
- [28] E. Brecht, W.W. Schmal, H. Fuess, S. Schmenn, N.H. Anderson, B. Lebeck, Th. Wolf, *Phys. Rev. B* 56 (1997) 940.
- [29] M.V. Eremin, I. Eremin, A.V. Terzi, *Phys. Rev. B* 66 (2002) 104524.